THE JOURNAL OF BIOLOGICAL CHEMISTRY VOL. 282, NO. 32, pp. 23337–23347, August 10, 2007

Fibroblasts Derive from Hepatocytes in Liver Fibrosis via Epithelial to Mesenchymal Transition*

Received for publication, January 8, 2007, and in revised form, June 6, 2007 Published, JBC Papers in Press, June 11, 2007, DOI 10.1074/jbc.M700194200

Michael Zeisberg[‡1,2], **Changqing Yang**[‡1,3], **Margot Martino**[‡], **Michael B. Duncan**[‡4], **Florian Rieder**[‡], **Harikrishna Tanjore**[‡], **and Raghu Kalluri**[‡§¶5]

From the [‡]*Division of Matrix Biology, Department of Medicine, Beth Israel Deaconess Medical Center and Harvard Medical School, Boston, Massachussetts 02215, the* [§]*Department of Biological Chemistry and Molecular Pharmacology, Harvard Medical School, Boston, Massachusetts 02215, and the* [¶]*Harvard-MIT Division of Health Sciences and Technology, Boston, Massachusetts 02215*

Activated fibroblasts are key contributors to the fibrotic extracellular matrix accumulation during liver fibrosis. The origin of such fibroblasts is still debated, although several studies point to stellate cells as the principal source. The role of adult hepatocytes as contributors to the accumulation of fibroblasts in the fibrotic liver is yet undetermined. Here, we provide evidence that the pro-fibrotic growth factor, TGF-β1, induces adult mouse hepatocytes to undergo phenotypic and functional changes typical of epithelial to mesenchymal transition (EMT). We perform lineage-tracing experiments using *AlbCre.* R26R*stop*lacZ double transgenic mice to demonstrate that hepatocytes which undergo EMT contribute substantially to the population of FSP1-positive fibroblasts in CCL_4-induced liver fibrosis. Furthermore, we demonstrate that bone morphogenic protein-7 (BMP7), a member of the TGFβ superfamily, which is known to antagonize TGFβ signaling, significantly inhibits progression of liver fibrosis in these mice. BMP7 treatment abolishes EMT-derived fibroblasts, suggesting that the therapeutic effect of BMP7 was at least partially due to the inhibition of EMT. These results provide direct evidence for the functional involvement of adult hepatocytes in the accumulation of activated fibroblasts in the fibrotic liver. Furthermore, our findings suggest that EMT is a promising therapeutic target for the attenuation of liver fibrosis.

Liver cirrhosis is still the sixth most common cause of death among United States citizens from ages 25 to 64 (1). Cirrhosis of the liver and its functional loss, which is caused by a progressive fibrosis, occurs due to a variety of insults, such as viral hepatitis, metabolic or autoimmune diseases, toxic injury, or congenital abnormalities (1–3). Fibrosis in the liver, as with fibrosis in other organs such as lung, kidney, heart, or skin, is described as excessive deposition of extracellular matrix (ECM),[6] which leads to the destruction of organ structure and impairment of organ function. Activated fibroblasts are key mediators of organ fibrosis. In the fibrotic liver, such activated fibroblasts are considered to derive via activation and proliferation of resident stellate cells and periportal fibroblasts (1, 2, 4–9). Because specific treatments to halt progressive fibrosis of the liver are not yet available, further understanding of the underlying pathogenic mechanisms involved in the accumulation of scar-forming fibroblasts is required.

Evidence is evolving that fibroblasts are more heterogeneous than traditionally thought (10) and recent studies reveal additional mechanisms such as recruitment of bone marrow-derived cells and conversion of resident epithelia as contributors to the accumulation of activated fibroblasts in fibrotic tissues (10, 11). In this study, we attempted to gain further insights into the role of adult hepatocytes, the parenchymal epithelial cells of the liver, in the accumulation of fibroblasts in the inflamed liver. A direct contribution of hepatocytes to liver fibrosis is considered to be relatively minor, even though hepatocytes perform the majority of liver associated functions and constitute more than 80% of the liver cellular mass (1, 12). Therefore, we tested the hypothesis that hepatocytes could directly contribute to the accumulation of activated fibroblasts during liver fibrosis by actively engaging in cellular transition.

Epithelial to mesenchymal transition (EMT) is defined as a process in which epithelial cells loose their phenotypic characteristics and acquire typical features of mesenchymal cells such as fibroblasts (13, 14) (15). Plasticity resulting in cells shifting between epithelial and mesenchymal phenotypes is essential during embryonic development, as it permits anchored epithelial cells to re-orient their phenotypic characteristics in a developing organism (16). In adults, EMT involving resident epithelia is speculated to occur in response to injury, which protects them from cell death by serving as an additional source of fibro-

* This study was funded in part by the Espinosa Fibrosis Fund, a research grant from the Johnson & Johnson Companies, Research Grants DK62987, DK55001, DK61688, and AI53194 (to R. K.) from the National Institutes of Health, and a research fund from the Beth Israel Deaconess Medical Center for the Division of Matrix Biology. The first evidence for EMT involving adult primary hepatocytes was first reported by our laboratory at the 2003 Digestive Disease Week (DDW) meeting in Orlando, Florida. The costs of publication of this article were defrayed in part by the payment of page charges. This article must therefore be hereby marked "*advertisement*" in accordance with 18 U.S.C. Section 1734 solely to indicate this fact.
[1] Both authors contributed equally to this report.
[2] Funded by Grant 5K08DK074558-01 from the National Institutes of Health and the ASN Carl W. Gottschalk Award 2006.
[3] Funded by a postdoctoral fellowship derived from the Espinosa Fibrosis Fund and BIDMC Liver Center.
[4] Funded by National Institutes of Health Grant DK055001-07S1.
[5] To whom correspondence should be addressed: Dept. of Medicine, Beth Israel Deaconess Medical Center, Harvard Medical School, 330 Brookline Ave., RW514, Boston, MA 02215. Tel.: 617-667-0445; Fax: 617-975-5663; E-mail: rkalluri@bidmc.harvard.edu.

[6] The abbreviations used are: ECM, extracellular matrix; EMT, epithelial to mesenchymal transition; TGF, transforming growth factor; ELISA, enzyme-linked immunoassay; BMP, bone morphogenic protein; FSP1, fibroblast-specific protein-1; β-gal, β-galactosidase; αSMA, α-smooth muscle actin.

blasts, which are essential for the repair of injured tissue (11, 17, 18). During organ fibrosis, such as in the kidney or lung, conversion of epithelium into fibroblasts is considered detrimental, as it leads to the disruption of polarized epithelial layers and an increase in the fibrotic scar formation (17). In the adult liver, however, evidence for EMT involving hepatocytes is lacking. Recent studies suggest that EMT is a promising therapeutic target for inhibition or even reversal of fibrosis in the kidney (19, 20). In the fetal liver, hepatocytes are detected in various intermediate stages of EMT (defined as cells which co-express mesenchymal and also hepatocyte markers), further suggesting that at least during fetal development, hepatocytes can contribute to the emergence of cells with mesenchymal features (21, 22).

In the present study, we demonstrate that in addition to αSMA-positive myofibroblasts a second population of fibroblast-specific protein-1 (FSP1) positive fibroblasts contribute to the progression of liver fibrosis. We demonstrate for the first time that under the influence of TGF-β1 up to 45% of FSP1-positive fibroblasts derive from hepatocytes via EMT. We further demonstrate that administration of BMP7, a growth factor which is known to inhibit TGF-β1 action, inhibits progression of liver fibrosis and that such protection of the liver is partially mediated by prevention of EMT.

EXPERIMENTAL PROCEDURES

Materials—Recombinant human TGF-β1 and antibodies specific to mouse albumin were purchased from R&D Systems (Minneapolis, MN). Matrigel™, mouse type I collagen, and mouse type IV collagen were obtained from BD Biosciences (Bedford, MA). E-cadherin antibodies were purchased from Sigma-Aldrich. Alexa Fluor 488 and 568-labeled secondary antibodies were purchased from Molecular Probes (West Grove, PA). FSP1 antibodies are a gift from Dr. Eric G. Neilson.

Mice—C57BL/6 mice and CD1 mice were purchased from Charles River Laboratories (Cambridge, MA). *Alb1Cre* and R26Rstop*lacZ* transgenes were described previously (23, 24). In *AlbCre* and R26Rstop*lacZ* double transgenic mice, the stop codon of the lacZ gene, which is ubiquitously expressed under the control of the Rosa promoter, is deleted upon expression of Cre recombinase. Because in *AlbCre* mice, the Cre recombinase is expressed in hepatocytes, the *lacZ* gene is irreversibly expressed in all cells of hepatocyte origin in livers of *AlbCre;* R26Rstop*lacZ* double transgenic mice. To obtain *Alb1Cre; R26stoplacZ mice* matings were set up between *Alb*Cre-positive and homozygous R26Rstop*lacZ* mice. All mice were housed under standard conditions in the animal facility of the BIDMC. All experiments were conducted with the ethical approval of the institutional Animal Care and Use Committee of the Beth Israel Deaconess Medical Center.

Administration of rhBMP7—rhBMP7 (300 μg/kg) was administered intraperitoneally to mice every other day, starting 1 day prior (prevention) or 2 weeks after the first injection of CCl_4 (intervention) for the entire duration of the study (6 weeks). rhBMP7 was a research gift from Curis, Inc.

Isolation of Primary Mouse Hepatocytes—We used a new method (modified) to isolate primary mouse hepatocytes with insignificant contamination with stellate cells (25). Livers of C57BL/6 mice were perfused through the portal vein with HBSS buffer, which contained 10 units/ml heparin. The livers were removed from the mice and were perfused with HBSS buffer, containing 0.0025% type I collagenase and 0.075% $CaCl_2$ for 30 min at 25 °C. Then they were triturated and digested for an additional 30 min at 25 °C in HBSS, containing type I collagenase. The liver suspension was filtered through an 80 micron sieve and the collected solution was sedimented for 20 min. To avoid contamination of hepatocytes with stellate cells, we used an additional purification step. The cell pellet was resuspended in 10 ml of Dulbecco's modified Eagle's medium and an equal volume of Nycodenz (18% w/v) was added. The suspension was then centrifuged for 30 min at 1,200 × *g*. The interface containing stellate cells was discarded, and the sedimented hepatocytes were washed three times in Ham F12 medium containing 10% fetal bovine serum. The hepatocytes were then added onto a Matrigel-coated dish in F12 medium, containing 10% fetal bovine serum and 2 μg/ml insulin. The purity of the hepatocytes was screened by morphology of viable cells and confirmed by albumin staining. Primary hepatocyte cultures utilized in the present study were 97% pure as determined by morphology and immunocytochemistry. To exclude potential contamination by significant numbers of stellate cells, the cells were double-stained for the expression of albumin and FSP1. About 97% of all cells were just positive for albumin expression.

Induction of EMT in Vitro—Primary mouse hepatocytes (1×10^6/dish) were cultured for 48 h in F12 medium containing 10% fetal bovine serum and 2 μg/ml insulin until they had adhered. To induce EMT, the media was replaced with F12 media supplemented with 0.5% fetal bovine serum and 2 μg/ml insulin containing TGF-β1 for 48 h.

Migration Assay—Migration assays using a Boyden chamber were performed as previously described (26). The bottom wells of chamber were filled with F12 medium containing supplements according to the specific experimental protocol. 20,000 freshly isolated hepatocytes were added to each well in the upper chamber and the Boyden chamber was incubated at 37 °C for 6 h or 48 h, to allow possible migration of cells into the lower chamber. Membranes were stained with Hema3® stain according to the manufacturer's recommendations (Biochemical Sciences, Inc., Swedesboro, NJ). Cells that migrated through the membrane were counted using a counting grid, which was fitted into an eyepiece of a phase contrast microscope. All experiments were repeated at least three times.

Immunocytochemistry—EMT in primary mouse hepatocytes was visualized by immunofluorescent double staining with antibodies to albumin, FSP1, β-galactosidase and E-cadherin as described with minor modifications (27). Cells were fixed with acetone at 4 °C and incubated for 1 h with the primary antibodies. For E-cadherin/FspI double staining experiments, the cells were fixed for 20 min in ice-cold acetone, and the slides were incubated with the primary antibodies at 4 °C overnight. Cells were then washed again and incubated for 45 min at room temperature with Alexa Fluor 488- and Alexa Fluor 568-conjugated secondary antibodies. The nuclei were counterstained using TOPRO3, and sections were covered using Vectashield mounting media (Vector, Burlingame, CA). Staining was analyzed using a confocal microscope.

CCl_4-induced Liver Fibrosis—Liver fibrosis was induced by CCl_4 injection in mice as previously described (28). Briefly, C57BL/6 mice were injected with CCl_4 (250 μl of 20% v/v CCl_4) intraperitoneally twice a week. Mice were sacrificed after 4 weeks and their livers were harvested. The tissue was fixed in 10% formalin for histopathology or snap-frozen in Tissue-Tek™ for immunohistochemistry. We started treatment with 300 μg/kg rhBMP7, which was determined as the optimum dose in several animal studies the day before the first CCl_4 injection (prevention study) or 2 weeks after the first CCl_4 injection (intervention trial) as previously reported (19, 29). RhBMP7 was administered by intraperitoneal injections every other day until week six ($n = 6$ mice per group), when the mice were sacrificed and livers and serum were obtained.

Tissue Preparation and Histological Assessment of Liver Fibrosis—The livers were removed, washed in phosphate-buffered saline, and cut in cross-sections of about 3 mm. Of each liver one piece of tissue was fixed in 4% paraformaldehyde, and embedded in paraffin for morphometric analysis. The other piece was embedded in OCT and snap-frozen in liquid nitrogen to perform immunohistochemistry. Paraffin embedded tissue was cut into 5-μm thick cross-sections, and sections were stained with hematoxylin and eosin, and Masson's trichrome. To quantify liver fibrosis, three independent Masson's trichrome-stained sections were analyzed from each mouse, using a counting grid. The percent area of liver fibrosis was calculated as previously described (30).

Immunofluorescence Staining—We performed immunofluorescence staining as previously described (29). Frozen tissue was cut into 5-μm thick cross-sections which were fixed in 100% acetone at −20 °C for 10 min. We incubated the sections with primary antibodies FSP-1 (31), LacZ (Alpha Diagnostics), Collagen III (Southern Biotechnology) or α-smooth muscle actin (Sigma) at 4 °C overnight. After the sections were washed with Tris-buffered saline, they were subsequently stained with secondary antibodies. The nuclei were counterstained with DAPI (Vectashield) for fluorescence microscopy or with TOPRO-3 (Molecular Probes) for confocal microscopy. FSP-1 antibody was a gift from E. G. Neilson (Vanderbilt University, Nashville, TN).

Staining Analysis—Relative stained area was assessed using NIH ImageJ software as described in our previous publications (32). For quantification of FSP1-positive and FSP1/β-gal double-positive cells a total of 1000 cells were evaluated for each group.

LacZ Staining—Liver tissue (~1 mm^3) were fixed in 4% PFA at 4 °C for 60 min, washed three times in phosphate-buffered saline and then incubated at 37 °C in 1 mg/ml X-gal (Sigma), 5 mM potassium ferrocyanide, 5 mM potassium ferricyanide, 2 mM $MgCl_2$, 0.2% Nonidet P-40, and 0.1% sodium deoxycholate in phosphate-buffered saline for 72 h. Tissues were mounted in paraffin and counterstained with eosin.

Immunohistochemistry—Immunohistochemistry of 10% formaldehyde-fixed, paraffin-embedded liver sections was performed as described previously with minor modifications (33). Briefly, sections were de-paraffinized and microwaved in Antigen Unmasking Solution (Vector Laboratories, Burlingame, CA) according to the manufacturer's recommendations. Immunohistochemical staining was performed using primary antibodies to Alk2 (R&D systems), Alk3 (R&D Systems) and Alk-6 (Santa Cruz Biotechnology) and the Vector Alkaline-phosphatase immunoassay kit (Vector Laboratories). Positive staining was visualized with the Vector Alkaline Phosphatase Substrate Kit I, and sections were counterstained with methylene-green.

Albumin ELISA—Serum albumin was determined using an ELISA kit (Alpha Diagnostics, San Antonio, TX) according to the manufacturer's recommendations. Briefly, serum samples were diluted 1:70,000 in sample diluent. The precoated ELISA plate was incubated with 20 μl of the diluted samples for 60 min at room temperature, followed by vigorous washing and incubation with a secondary antibody-horseradish peroxidase conjugate solution. After washing horseradish peroxidase-substrate solution was added, and color development was assessed by measurement of the absorbance at 450 nm using an ELISA reader. The serum albumin concentration was calculated by plotting the net absorbance values against appropriate albumin standard concentrations. The normal value for serum albumin in C57BL/6 mice, assessed by testing 25 different adult C57BL/6 mice sera samples, was 20.3 mg/ml.

Statistical Analysis—Results are expressed as means ± S.E. Multiple comparisons were performed by one-way analysis of variance. p values lower than 0.05 were considered significant.

RESULTS

Accumulation of FSP1-positive Fibroblasts in Liver Fibrosis—The key mediators of liver fibrosis are activated fibroblasts, which are traditionally detected by means of α-smooth muscle actin (αSMA) expression (1, 34). However, recent studies in the setting of fibrosis in kidney, solid tumors, lung, and skin reveal that the heterogeneity of activated fibroblasts is greater than commonly believed (35). FSP1-positive fibroblasts (characterized by their expression of fibroblast specific protein 1, a member of the S100 family of calcium-binding proteins), is one class of fibroblasts present in many tissues (17, 36). To gain insights into the contribution of FSP1-positive fibroblasts to liver fibrosis, we established a disease progression curve by sacrificing cohorts of mice with CCl_4-induced liver fibrosis at various time points after initial injection of CCl_4 (2 weeks, 4 weeks, 6 weeks, $n = 6$ in each group) (Fig. 1). In control livers, few FSP1-positive fibroblasts are noticed, predominantly surrounding central veins and within the periportal region (Fig. 1*A*). Immunofluorescence double-labeling experiments using antibodies specific to FSP1 and Collagen III revealed that FSP1-positive fibroblasts accumulate during fibrosis progression, predominantly in areas of collagen III deposition (Fig. 1, *A–C*). Experiments in which liver sections were double-labeled with antibodies to αSMA and FSP1 reveal that these two markers rarely co-localize (Fig. 1, *D–I*). In control livers, αSMA expression is restricted to vascular smooth muscle cells, distinct from the FSP1-positive cells (Fig. 1, *D–G*). During early stages of liver fibrosis (after 2 weeks of CCl_4 administration), both αSMA-positive cells and FSP1-positive cells increase in numbers, but do not overlap (Fig. 1, *E* and *H*). During advanced stages of fibrosis (after 6 weeks of CCl_4 administration), both αSMA-positive cells and FSP1-positive cells substantially accumulate in the areas of fibrotic septae

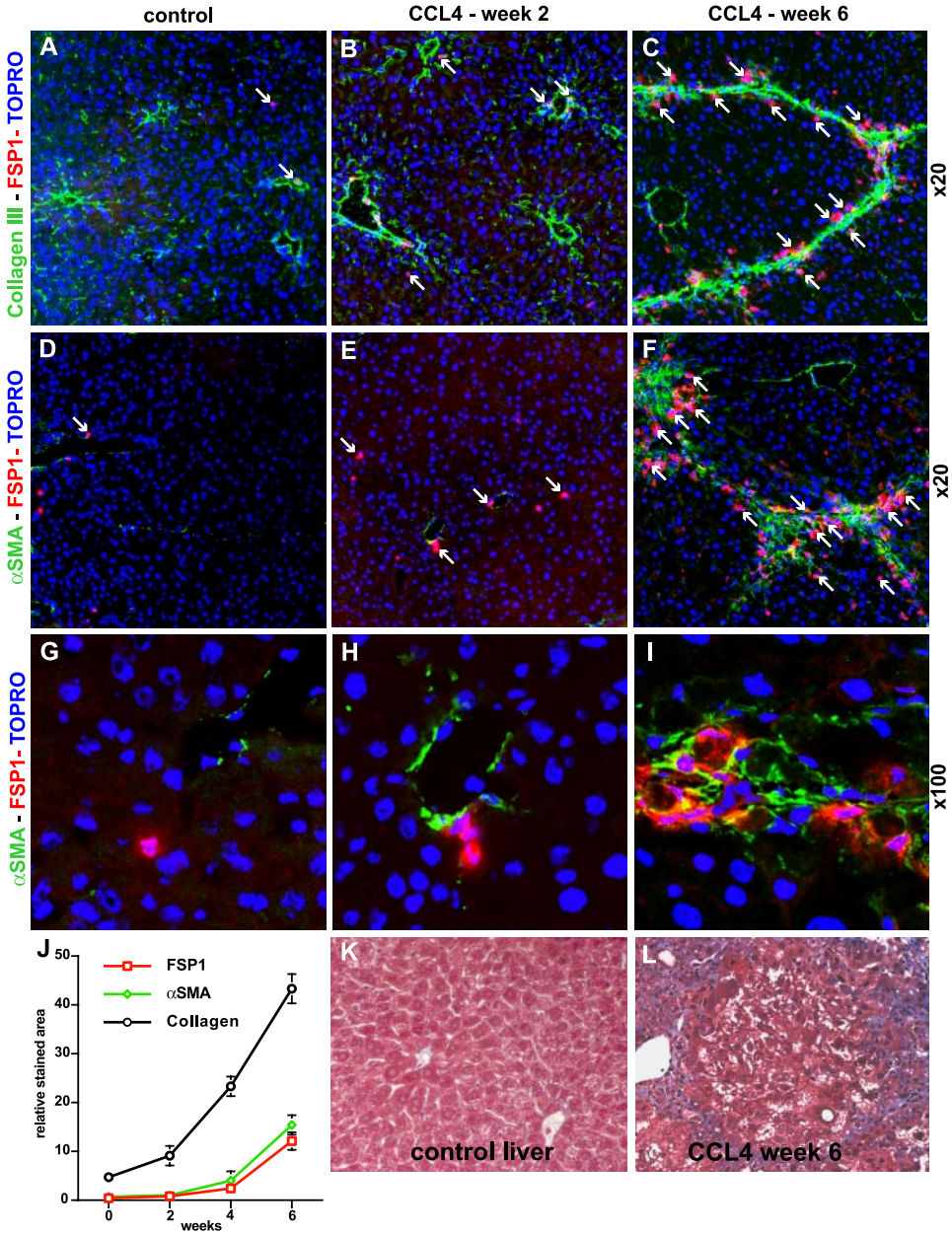

FIGURE 1. **Contribution of FSP1-positive fibroblasts to liver fibrosis.** Liver fibrosis was induced by CCl_4 injection over 6 weeks in C57BL/6 mice. Cohorts of mice were sacrificed at 0 weeks (control), 2 weeks, 4 weeks, and 6 weeks after the initial CCl_4 injection to document disease progression. *A–C*, collagen III-FSP1 double-labeling. Liver sections were stained with antibodies specific for collagen III (*green*) and FSP1 (*red*, *arrows*). The pictures display representative photomicrographs of each group. Accumulation of collagen III was associated with accumulation of FSP1-positve fibroblasts (*arrows*). *D–I*. FSP1-αSMA double labeling. The pictures display representative photomicrographs of liver sections that were labeled with antibodies specific for αSMA (*green*) and FSP1 (*red*) at an original magnification of ×20 (*D–F*) and ×100 (*G–I*). In control livers (*D* and *G*) αSMA-labeling was restricted to larger vessels. Progression of fibrosis correlated with accumulation of αSMA-positive as well as FSP1-positive cells. Few cells positive for both αSMA and FSP1 were only present in advanced stages of fibrosis (*I*, *yellow staining*). *J*, graph summarizes quantitative analysis of collagen III, αSMA, and FSP1 staining using NIHI ImageJ software in each group. *K* and *L*, Masson Trichrome staining. The picture in *panel K* displays a representative MTS-stained control liver (original magnification ×20). After 6 weeks of CCl_4 administration, livers displayed substantial fibrotic lesions (*L*).

(Fig. 1, *F* and *I*). However, only ~10% of FSP1-positive cells are also positive for αSMA (Fig. 1*I*).

TGF-β1 Induces EMT in Primary Mouse Hepatocytes—FSP1-positive fibroblasts have been well-characterized in fibrogenesis in kidney, lung, and solid tumors. As opposed to αSMA fibroblasts, which predominantly derive via activation of resident stellate cells and fibroblasts or via shedding from vascular smooth muscle cells, FSP1-positive fibroblasts have been shown to derive by a significant extend from resident epithelia via epithelial-mesenchymal transition. We hypothesized that hepatocytes could contribute to the pool of FSP1-positive fibroblasts in the setting of liver fibrosis. TGF-β1 is considered to be the principal mediator of liver fibrosis (37, 38), and it is the most potent inducer of EMT in different organ systems (39, 40). Therefore, we tested the capacity of TGF-β1 to induce EMT in primary cultures of adult mouse hepatocytes (41).

In the absence of growth factors, 97% of cells isolated from adult mouse livers were albumin-positive hepatocytes (see methods). FSP1 staining and αSMA staining was negligible (less than 3% of the cells) (Fig. 2*A–C*). After exposure of these primary mouse hepatocytes to 3 ng/ml of human TGF-β1 for 48 h (optimum stimulus for the induction of EMT in several different epithelial systems), the albumin-positive cells also uniformly express FSP1 (Fig. 2, *D–F*). The negligible number of albumin negative cells (< 3% of the cells) did not increase. After 96 h of TGF-β1 incubation, albumin staining was lost and the cells were uniformly spindle-shaped and positive for FSP1, typical of an EMT-derived fibroblast (Fig. 2, *G–K*). Gain of FSP1 expression upon exposure to TGF-β1 also coincided with decreased staining for the epithelial marker E-cadherin (Fig. 2, *L–Q*) The findings suggest that after 48 h of TGF-β1 incubation an intermediate phenotype (positive staining for both the hepatocyte marker and fibroblast marker) is observed, whereas after 96 h a more complete EMT occurs.

We next confirmed that the observed phenotypic change was indeed reflective of an EMT (loss of epithelial properties combined with gain of functional fibroblast properties) as opposed to hepatocyte de-differentiation (loss of hepatocyte properties). Migration is a hallmark feature of activated fibroblasts, which enables them to fulfill their physiological function during wound repair by quickly appearing at the site of injury (42), and

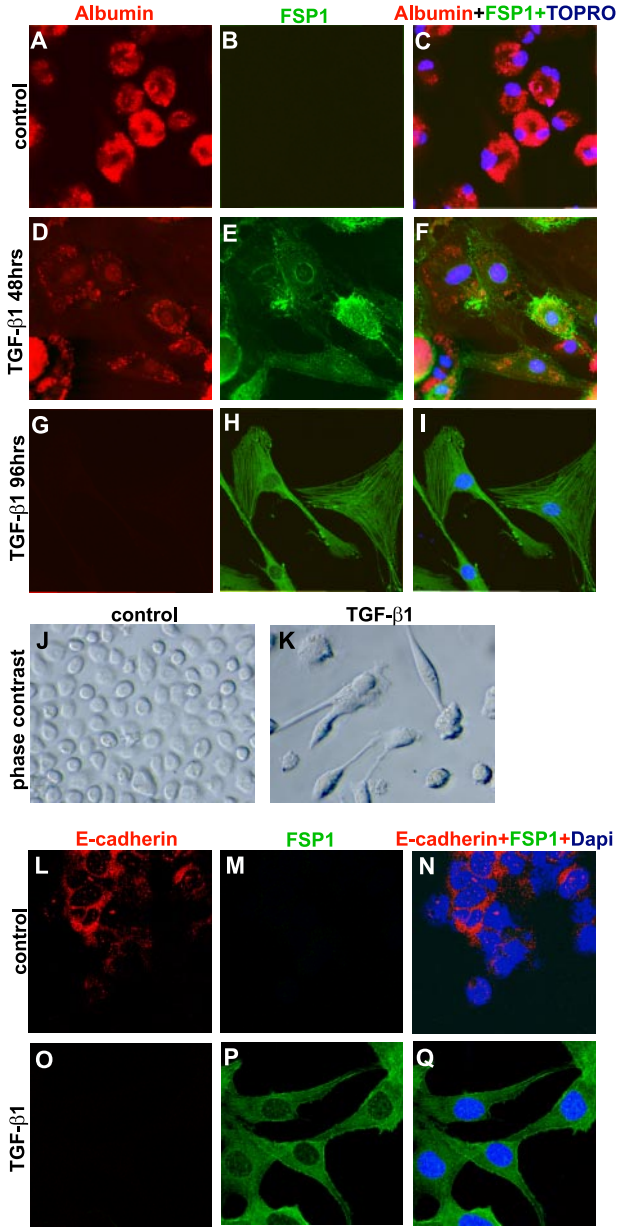

FIGURE 2. **De novo FSP1 expression in albumin-positive hepatocytes.** *A–I*, to demonstrate the induction of EMT, primary mouse hepatocytes were stimulated with TGF-β1(3 ng/ml) and double-labeled with antibodies specific for albumin (hepatocyte marker) and FSP1 (fibroblast marker) after 48 h and 96 h. Nuclei were visualized using TOPRO-3 staining. The pictures display representative photomicrographs, which were acquired by confocal microscopy at an original magnification of $\times$60. Whereas FSP1 staining was absent in control hepatocytes (*A–C*), hepatocytes were positive for both albumin and FSP1 after 48 h (*F*). After 96 h, albumin staining was neglible (*G–I*). *J* and *K*, light microscopy. While primary mouse hepatocytes displayed a homogenous round-shaped appearance (*J*), stimulation with TGF-β1 induced an acquisition of a fibroblast-like phenotype (*K*). *L–Q*, E-cadherin/FSP1 double staining. Normal hepatocytes express E-cadherin (*red*). Incubation of primary hepatocytes with TGF-β1 induces FSP1 expression (*green*) associated with decreased E-cadherin staining.

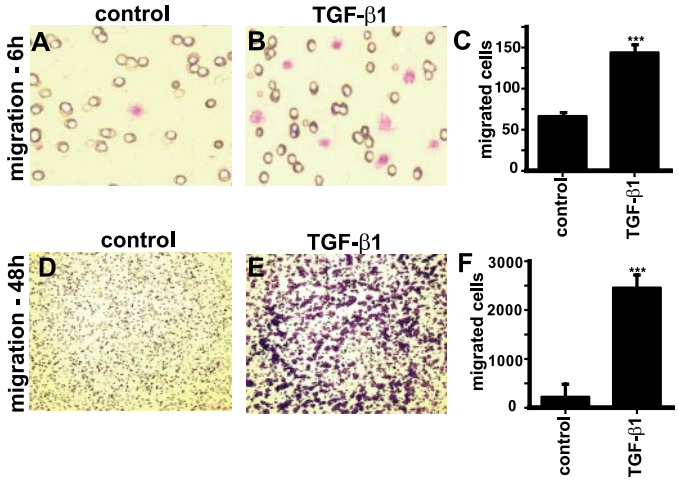

FIGURE 3. **Migration of primary hepatocytes.** *A–C*, migration of hepatocytes after 6 h. Representative light microscopy pictures displaying the stained cells that migrated to the bottom side bottom side of the polyvinylidene difluoride membrane at a magnification of $\times$40. When TGF-β1 (3 ng/ml) was added into the upper chamber (*B*) and migratory activity was increased as compared with the control (*A*). *C*, the graph summarizes the average total number of cells that migrated into the bottom compartment. The average of a total of three independent experiments is displayed. *D–F*, migration of hepatocytes after 48 h. The pictures display slides after 48 h of migration without stimulation with TGF-β1 (*D*) and after stimulation with TGF-β1 (*E*) at an original magnification of $\times$100. The graph summarizes the average total number of cells that migrated into the bottom compartment after 48 h (*F*). ***, $p < 0.001$.

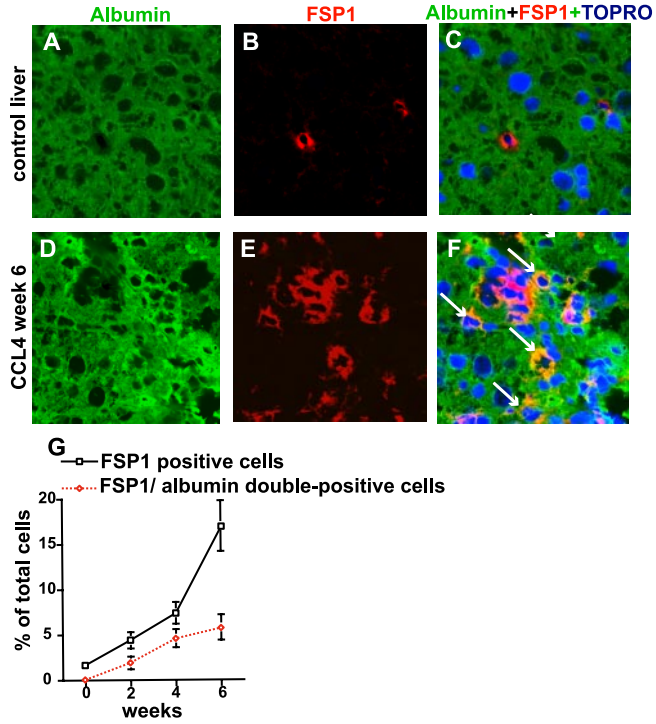

FIGURE 4. **Albumin-FSP1 double-positive cells in liver fibrosis.** Liver fibrosis was induced by bi-weekly injection of CCl_4 for 6 weeks. Livers were stained with antibodies to FSP1 (*red*) and albumin (*green*). Nuclei were visualized using TOPRO-3 counterstaining (*blue*). Photomicrographs were obtained using a confocal microscope at an original magnification of $\times$100. *A–C*, albumin-FSP1 double-labeling of control livers. There was no co-localization of albumin and FSP1-labeling. *D–F*, albumin-FSP1 double-positive cells in liver fibrosis. Co-localization was detected by overlaying the *red*, *green*, and *blue panels* (*right pictures*). The *arrows* point to round-shaped albumin-positive cells that expressed FSP1 (*F*), suggesting EMT involving hepatocytes. FSP1-positive fibroblasts and albumin/FSP1 double-positive cells were quantified at 0, 2, 4, and 6 weeks of CCl_4 injection. The graph summarizes average numbers of FSP1 positive and albumin/FSP1 double-positive cells at each time point (*G*).

like other cells of epithelial lineage, hepatocytes are immobile and tightly integrated into the epithelial cell layer (43). In order to provide further evidence that TGF-β1 induces a gain of fibroblast-like function involving hepatocytes, we evaluated migratory capacity of primary mouse hepatocytes. We used a two-compartment Boyden chamber, which utilized a polycar-

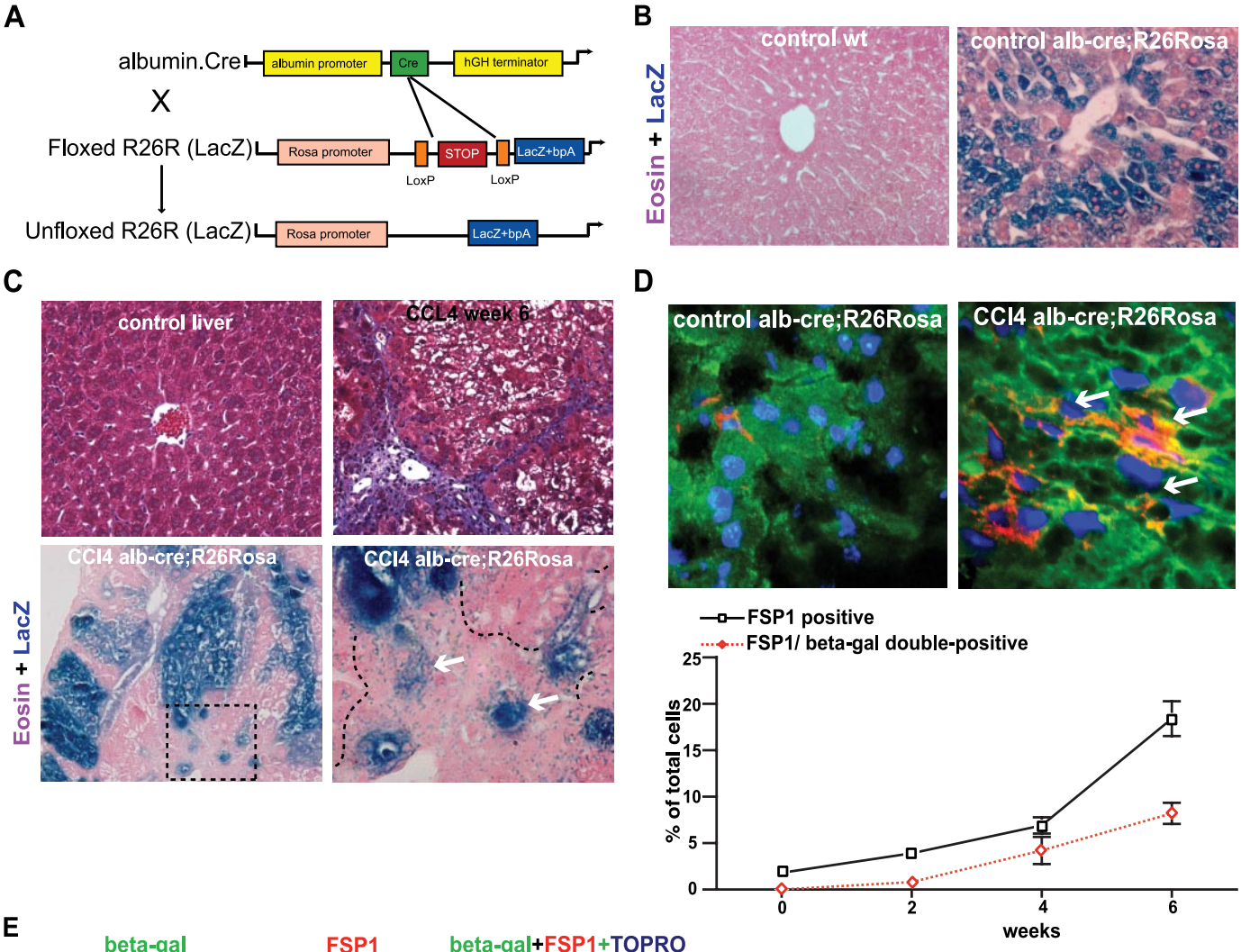

bonate membrane coated with type IV collagen and type I collagen (both up-regulated during fibrosis) to study migration. The migration rate was assessed after 6 h and after 48 h of stimulation with TGF-β1 (44). After stimulation with TGF-β1 for 6-h migration of cells into the bottom chamber was already increased as compared with the untreated control. (2.2-fold increase compared with control) (Fig. 3, *A–C*). The total number of cells that had migrated after 6 h (an average of 144 cells out of a total 20,000 seeded cells) was rather small at this time point. Incubation with TGF-β1 for 48 h (allowing hepatocytes enough to undergo EMT) induced significantly increased migration of primary hepatocytes into the bottom compartment (an average of 2460 cells out of 20,000 originally seeded hepatocytes) (Fig. 3, *D–F*). In summary, these results suggest that EMT of primary hepatocytes is associated with a significantly enhanced motility.

Evidence for EMT Involving Adult Hepatocytes in a Mouse Model for Liver Fibrosis—Our studies suggest that hepatocytes could acquire a fibroblast-like phenotype in the *in vitro* experiments. Next, we evaluated the presence of hepatocyte-derived fibroblasts in mouse models of liver fibrosis. We first evaluated for possible EMT involving hepatocytes in the mouse model of CCl_4-induced liver fibrosis. In this model, TGF-β1-dependent liver fibrosis begins 2 weeks post-CCl_4 injection, eventually leading to severe liver fibrosis after 6 weeks (28). Among the accumulated FSP1-positive fibroblasts, up to 60% (after 2 weeks of CCl_4 injection) co-labeled with albumin (Fig. 4, *A–G*), consistent with the intermediate phenotype of EMT observed in our *in vitro* studies. In the advanced stages of fibrosis (after 6 weeks of CCl_4 injection), 17% of all cells were FSP1 positive and up to 28% of these FSP1 positive fibroblasts were positive for albumin, indicating their hepatocyte origin. While these studies demonstrate the presence of hepatocytes, which reflect a possible intermediate transitional stage of EMT (positive for both the fibroblast marker FSP1 and the hepatocyte marker albumin), these studies could not demonstrate a complete conversion of hepatocytes to fibroblasts, because the methodology design was insufficient to distinguish fibroblasts which potentially derive *de novo* from resident fibroblasts via proliferation, from those which are derived via EMT loss of albumin expression.

Genetic Lineage Tag Evidence for EMT Involving Hepatocytes during Liver Fibrosis—To provide further evidence for EMT involving hepatocytes during liver fibrosis, we next performed lineage analysis of fibroblasts recruited during fibrosis, using double transgenic mice which express Cre-recombinase under control of the albumin promoter (*AlbCre+*) and which also harbor an allele in which a STOP cassette flanked by two loxP sites is inserted between the R26Rosa promoter and the LacZ gene (R26Rstop*lacZ*) (Fig. 5*A*) (24, 45). The albumin gene is expressed by mature hepatocytes. In *AlbCre+* mice, the Cre recombinase is expressed under the Alb promoter and thus present in mature hepatocytes (45). In the R26Rstop*lacZ* indicator strain, the *LacZ* reporter gene is activated after Cre-mediated excision of a LoxP stop cassette (24). Therefore, in the *AlbCre;* R26Rstop*lacZ* double transgenic mice the *LacZ* gene remains activated in hepatocytes and in all cells with a previous hepatocyte origin, despite possible phenotype changes.

To investigate the contribution of EMT involving hepatocytes in liver fibrosis, CCl_4 was administered to *AlbCre;* R26Rstop*lacZ* adult mice. In the normal livers of *AlbCre;* R26Rstop*lacZ* mice, LacZ expression can be detected in ~70% of hepatocytes, whereas LacZ staining was completely absent in livers of *wt;* R26Rstop*lacZ* control mice (Fig. 5*B*). These results confirm previous studies, demonstrating a high specificity (no LacZ staining in cells other than hepatocytes, absence of staining in livers of AlbCre-negative control mice) albeit limited sensitivity (~70%) of this system (45). Administration of CCl_4 over a period of 6 weeks results in liver fibrosis similar to that observed in the wt C57BL6 mice (Fig. 5*C*). LacZ staining of fibrotic livers reveals several lacZ positive cells within fibrotic zones (Fig. 5*D*). Double-labeling of liver tissues with FSP1 antibodies (red fluorescence staining) and β-gal antibodies (green fluorescent staining) reveals that in fibrotic livers (after 6 weeks of CCL_4) 18.4% (+4.24%) of all cells were FSP1-positive and 8.2% (+1.13%). This means that up to 45% of FSP1-positive fibroblasts are also positive for β-gal, indicating that about half of FSP1-positive fibroblasts in liver fibrosis exhibit a hepatocyte imprint (Fig. 5*D*). To further verify that FSP1/β-gal double-positive cells were indeed representative of hepatocyte-derived fibroblasts, we isolated primary hepatocytes from *AlbCre;* R26Rstop*lacZ* mice and incubated them with TGF-β1. Hepatocytes derived from *AlbCre;* R26Rstop*lacZ* mice labeled positive for β-gal while they were negative for FSP1 in absence of TGF-β1. When TGF-β1 was added for 48 h, cells co-expressed FSP1 and β-gal (Fig. 5*E*), further supporting our analysis using anti-albumin antibodies in the previous experiments (Fig. 2, *D–F*). However, even after 96 h of TGF-β1 incubation, when albumin expression is lost in our earlier experiments (Fig. 2, *G–I*), the *AlbCre;* R26Rstop*lacZ* hepatocytes remain positive

FIGURE 5. **Lineage tracing of hepatocytes using *AlbCre;* R26Rstop*lacZ* mice.** *A*, schematic illustration. Crossing of *AlbCre*;wt mice with R26Rstop*lacZ* mice generates *AlbCre*$^+$; R26Rstop*lacZ* mice. Cre recombinase removes the STOP cassette from between the Rosa promoter and the *LacZ* gene in albumin-positive cells. In these cells the *LacZ* gene is constitutively expressed under control of the R26 Rosa promoter, even if albumin expression is lost. *B*, β-galactosidase staining. β-galactosidase staining was performed on livers from *AlbCre*$^-$; R26Rstop*lacZ* mice (left picture) and from *AlbCre*$^+$; R26Rstop*lacZ* mice. When this method is used, the presence of β-galactosidase (product of the *LacZ* gene) is indicated by a blue precipitate. The absence of blue staining in *wt*; R26Rstop*lacZ* mice indicates high specificity of the system. Approximately 70% of hepatocytes stain blue in *AlbCre*; R26Rstop*lacZ* livers. *C*, liver fibrosis in *AlbCre*; R26Rstop*lacZ* mice. *AlbCre*; R26Rstop*lacZ* mice received bi-weekly injections of CCl_4 for 6 weeks. MTS staining revealed liver fibrosis after 6 weeks. Beta galactosidase staining in fibrotic livers from *AlbCre*; R26Rstop*lacZ* mice revealed the presence of single β-gal-positive cells within fibrotic lesions. The *right panel* shows a higher magnification (×63) of the boxed region in the *left picture*. The *dotted line* in the *right picture* indicates the outer margin of the fibrotic area, the *arrows* indicate single β-gal-positive cells within the fibrotic lesion. *D*, β-gal/FSP1 double labeling *in vivo*. We performed immunofluorescence double labeling using antibodies specific to β-gal (*green*) and FSP1 (*red*). In fibrotic livers FSP1-positive cells were present that were also positive for β-gal, revealing their hepatocyte origin. The graph summarizes the average percentage of FSP1 positive fibroblasts and FSP1-β-galactosidase double-positive cells (hepatocyte-derived fibroblasts) per ×40 visual field. *E*, β-gal/FSP1 double labeling *in vitro*. Primary hepatocytes were isolated from *AlbCre*; R26Rstop*lacZ* mice and subjected to TGF-β1 for 96 h. Acquisition of a spindle shaped morphology was associated with *de novo* expression of FSP1. β-gal expression remained stable, demonstrating the hepatocyte origin of these cells. The photomicrographs were acquired using a confocal microscope at a magnification of ×60.

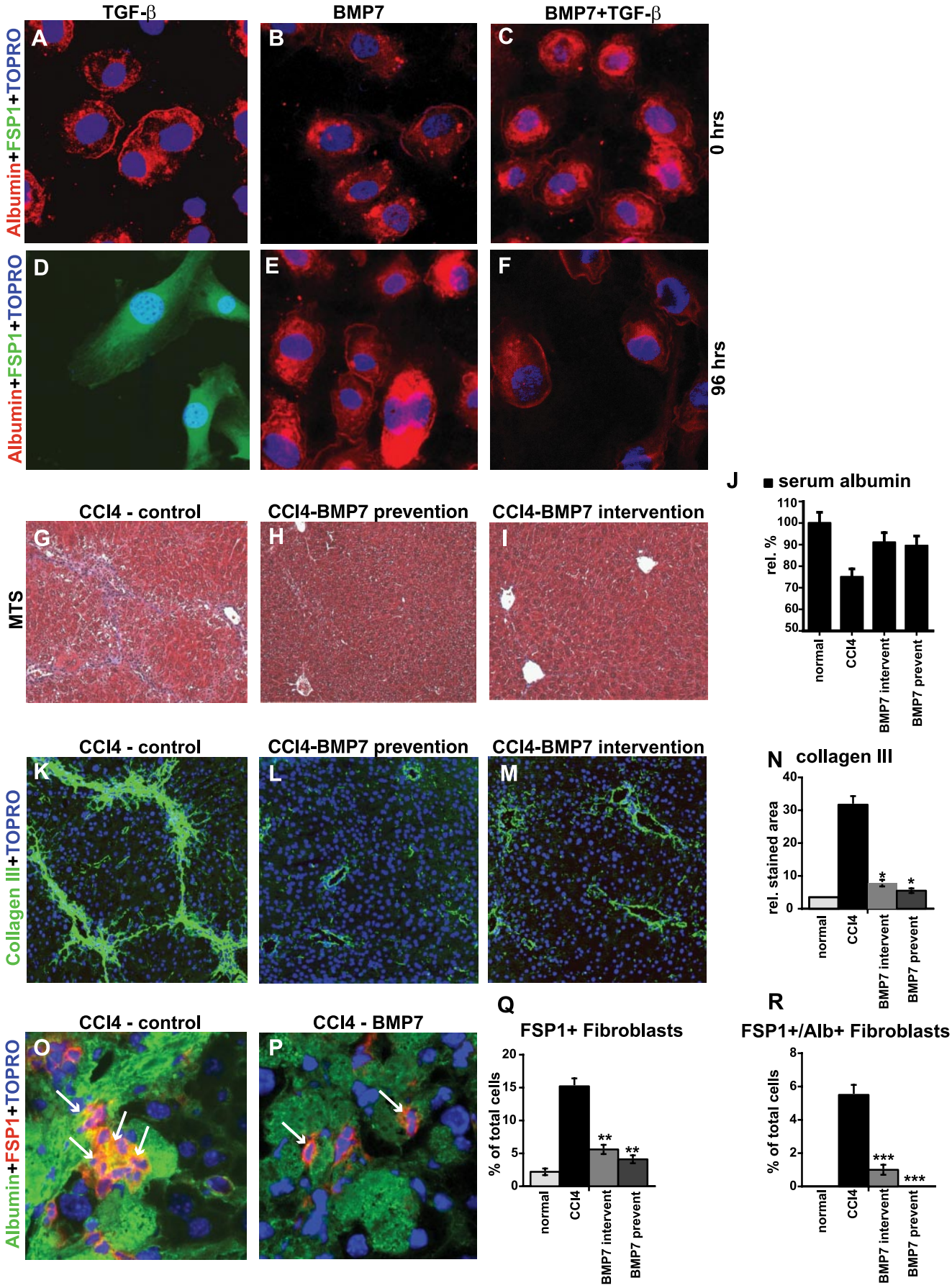

for β-gal (Fig. 5*E*), demonstrating the utility of the system to detect without ambiguity the contribution of hepatocytes in the generation of fibroblasts during liver fibrosis.

Prevention of EMT by Recombinant Human Bone Morphogenesis Protein-7 (rhBMP7) Inhibits Progression of Liver Fibrosis—BMP7 is a member of the TGF-β superfamily, involved in morphogenesis associated with a variety of organs. In the liver, BMP7, in concert with other BMPs such as BMP-4, regulates proliferation and differentiation of the liver bud, eventually leading to complete hepatocyte differentiation (46). Functional BMP7 receptors Alk3 and BMPR-II are expressed on adult hepatocytes, and because our data suggest that EMT involving hepatocytes is TGF-β1-dependent, we hypothesized that administration of recombinant human BMP7 (rhBMP7) could potentially inhibit progression of liver fibrosis by preventing EMT involving hepatocytes.

To test our hypothesis, we first subjected primary mouse hepatocytes to either TGF-β1, BMP7, or both TGF-β1 and BMP7 together and evaluated the impact on EMT by albumin and FSP1 co-labeling. Whereas TGF-β1 induced loss of albumin expression associated with newly acquired FSP1 expression (indicative of EMT), incubation with BMP7 (100 ng/ml) alone had no visible effect on hepatocyte phenotype (Fig. 6, *A–F*). However, BMP7 blocked TGF-β1 induced EMT when primary mouse hepatocytes were incubated with both TGF-β1 and BMP7 (Fig. 6, *A–F*).

To evaluate the therapeutic effect of rhBMP7 on hepatocytes *in vivo*, we used the CCl_4-induced liver fibrosis model in mice. We initiated treatment with rhBMP7 before induction of disease (prevention group) and also 2 weeks after the initial CCl_4 injection, when fibrotic lesions were established (intervention group). All animals were sacrificed after 6 weeks of disease and liver histology and serum albumin were compared between the BMP7 administered mice and the control mice. After 6 weeks, fibrotic lesions were substantially less in both the groups that received rhBMP7, as compared with the control group (Fig. 6, *G–N*). Improved histology was associated with improved liver function as determined by serum albumin levels (Fig. 6*J*). We next performed albumin/FSP1 double-labeling experiments to establish whether BMP7 inhibited EMT involving hepatocytes *in vivo*. Similar to our results obtained using primary mouse hepatocytes, cells that labeled for both albumin and FSP1 (indicative of EMT) were significantly diminished in rhBMP7 administered mice (Fig. 6, *O–R*).

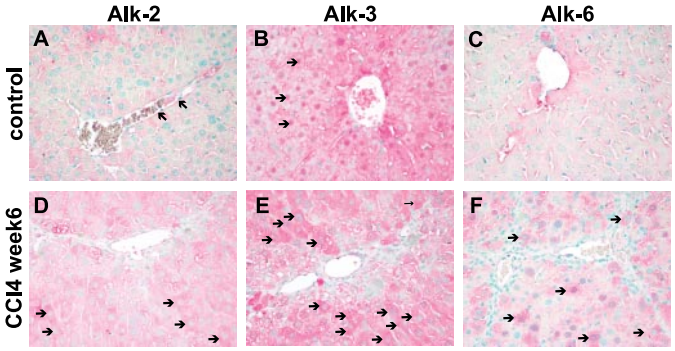

FIGURE 7. **Immunolocalization of BMP receptors in the liver.** Liver sections obtained from control mice (*A–C*) and mice that received CCL4 for 6 weeks (*D–F*) were stained with antibodies specific for ALk-2 (*A* and *D*), Alk-3 (*B* and *E*), and Alk-6 (*C* and *F*). Positive staining is indicated by *red* precipitate, nuclei are stained *green*. The pictures display representative photomicrographs of each group at an original magnification of ×40. In control livers, Alk-2 staining is predominantly located on endothelial cells (*A*, *arrows*), whereas Alk-2-positive hepatocytes are detected in fibrotic livers (*D*, *arrows*). In control livers robust Alk-3 staining is present, predominantly nuclei stain positive (*B*, *arrows*). In fibrotic livers, hepatocytes, and fibroblasts are Alk-3-positive (*E*, *arrows*). In fibrotic livers, few hepatocytes were also Alk-6 positive (*F*, *arrows*).

We further analyzed liver from control mice and from mice that received CCl4 for 6 weeks to gain insights into the receptors that mediate BMP7-action in hepatocytes. BMP7 is known to bind to the BMP type II receptor, which then forms complexes with specific type I serine-threonine kinase receptors (Alk receptors). BMP7 binds specifically to Alk-3 and Alk-6 and also to the activin receptor Alk-2 (47, 48). Immunohistochemistry using specific antibodies to Alk-2, Alk-3, and Alk-6 revealed that in control livers mainly Alk-3 is present on hepatocytes (Fig. 7, *A–C*). Interestingly, in fibrotic livers we also detected Alk-2 and Alk-6 expression on the hepatocytes (Fig. 7, *D–F*), suggesting that each of these receptors is potentially involved in mediating BMP7 action in the fibrotic liver.

DISCUSSION

Activated fibroblasts are the principal mediators of organ fibrosis. In the liver, several studies have unequivocally demonstrated that resident adult stellate cells can respond to many different forms of insult, including TGF-β1, by converting or contributing to activated fibroblasts seen in the injured liver (7, 49, 50). In addition, other cell types of the fibroblast lineage, such as portal fibroblasts or vascular myofibroblasts are also being recognized in this setting for their fibrogenic potential

FIGURE 6. **Inhibition of EMT by rhBMP7 is associated with amelioration of liver fibrosis.** *A–F*, albumin-FSP1 double labeling of primary hepatoctyes. Primary mouse hepatocytes were subjected to either TGF-β1, BMP7, or combination of TGF-β1 and BMP7 or to control media without growth factors. After 96 h, cells were stained using antibodies specific for FSP1 (*green*) and albumin (*red*). TGF-β1 induced FSP1 expression (*D*), whereas BMP7 alone had no effect on either albumin of FSP1 expression (*E*). In combination with TGF-β1, BMP7 prevented loss of albumin expression and FSP1 expression was not detected (*F*). *G–N*, prevention of liver fibrosis by BMP7. Livers from untreated control mice with CCl_4-induced liver disease, from mice that received rhBMP7 starting from day 0 of disease (prevention) and from mice that received treatment after 14 days of disease (intervention), were evaluated by MTS staining (*G–I*). The pictures in the *upper row* display representative MTS-stained liver sections of each group. Treatment with rhBMP7 resulted in substantial amelioration of fibrotic lesions (original magnification ×20). The graph summarizes serum albumin measurements for each group (*J*). The pictures in the *bottom row* display representative photomicrographs of liver sections that were labeled with antibodies to type III collagen (*green*) and TOPRO-3 nuclear counterstain (*blue*). *K–M*, the bar graph summarizes average type III collagen-stained area in each group (*N*). *O–R*, FSP1/albumin double staining. After 6 weeks of CCl_4-induced disease, livers from untreated control mice and from mice that received treatment with rhBMP7 for 6 weeks were stained with antibodies to FSP1 (*red*) and albumin (*green*) and the percentage of FSP1-positive fibroblasts and FSP1-positive/albumin double-positive cells (hepatocytes undergoing EMT) from total liver cells was assessed using a confocal microscope at an original magnification of ×100. In normal control livers and in BMP7-treated livers FSP1/albumin double-positive cells were absent. BMP7 treatment significantly decreased the number of FSP1-positive cells. The graphs summarize the quantification of six different livers, the pictures display representative staining for each group. *, $p < 0.01$; **, $p < 0.005$; ***, $p < 0.001$.

(7). In this regard, a contribution of damaged, injured or TGF-β1-influenced adult hepatocytes to this process is undetermined. Here we provide evidence that hepatocyte-derived fibroblasts are an additional and significant lineage of mesenchymal cells that contribute to progression of liver fibrosis.

In the present study we demonstrate that a substantial population (up to 45%) of FSP1-positive fibroblasts derives from hepatocytes via EMT. These results are similar to studies in the kidney, which report that about 40% of all fibroblasts are derived via EMT (17). While the importance of fibroblasts in the progression of liver fibrosis is undisputed, this study demonstrates that fibroblasts can increase in their number via different mechanisms. The relative individual contribution of stellate cell-derived fibroblasts, resident liver fibroblasts and hepatocyte-derived fibroblasts to the overall activated fibroblast population might be crucial for the progression of liver fibrosis. Whereas our studies demonstrate that hepatocytes contribute to the accumulation of fibroblasts by undergoing EMT, more extensive studies are required to determine if all hepatocytes, or just a select subpopulation, have the capacity to undergo EMT.

We demonstrate for the first time that administration of rhBMP7 effectively inhibits progression of fibrosis in the liver. The most striking effect of rhBMP7 administration was the almost complete absence of hepatocytes undergoing EMT. This confirms our working hypothesis that BMP7 is an inhibitor of TGF-β1-induced EMT. Additionally, strong correlation for the absence of EMT coupled with the inhibition of liver fibrosis suggests that EMT involving hepatocytes contributes significantly to the pathogenesis of liver fibrosis. We note that in rhBMP7-administered mice, the overall liver structure was improved associated with lesser number of inflammatory cells, decreased number of fibroblasts and less steatosis when compared with the livers from control mice. Additional studies are required to delineate underlying molecular mechanisms of the total therapeutic effect of BMP7, including its anti-inflammatory effect. BMP7 is not expressed in the liver, but the functional receptors for BMP7 are present on hepatocytes. We demonstrate that each of the three known BMP type I receptors are expressed on hepatocytes in diseased livers, and we previously demonstrated that in the setting of partial keratectomy neutralization of endogenous circulating BMP7 slows liver regeneration, suggesting that physiological levels of endogenous BMP7 have a putative role for hepatocytes in the setting of acute liver injury (51).

In summary, we demonstrate that hepatocytes can contribute to the accumulation of activated fibroblasts via EMT. EMT involving hepatocytes plays a functional role in the progression of fibrosis in two different mouse models for chronic liver disease. Inhibition of EMT by rhBMP7 leads to attenuation of liver fibrosis and improvement of liver function. Therefore, rhBMP7 may have a value as a therapeutic agent to control liver fibrosis.

Acknowledgments—We thank Curis, Inc. and the Johnson and Johnson Companies for recombinant human BMP7.

REFERENCES

1. Friedman, S. L. (2000) *J. Biol. Chem.* **275,** 2247–2250
2. Bataller, R., North, K. E., and Brenner, D. A. (2003) *Hepatology* **37,** 493–503
3. Tsukamoto, H. (1999) *Alcohol. Clin. Exp. Res.* **23,** 911–916
4. Li, D., and Friedman, S. L. (1999) *J. Gastroenterol. Hepatol.* **14,** 618–633
5. Gabele, E., Brenner, D. A., and Rippe, R. A. (2003) *Front Biosci.* **8,** D69–77
6. Brenner, D. A., Waterboer, T., Choi, S. K., Lindquist, J. N., Stefanovic, B., Burchardt, E., Yamauchi, M., Gillan, A., and Rippe, R. A. (2000) *J. Hepatol.* **32,** 32–38
7. Knittel, T., Kobold, D., Saile, B., Grundmann, A., Neubauer, K., Piscaglia, F., and Ramadori, G. (1999) *Gastroenterology* **117,** 1205–1221
8. Mehal, W. Z. (2006) *Gastroenterology* **130,** 600–603
9. Pavlova, A., Stuart, R. O., Pohl, M., and Nigam, S. K. (1999) *Am. J. Physiol.* **277,** F650–F663
10. Kalluri, R., and Zeisberg, M. (2006) *Nat. Rev. Cancer* **6,** 392–401
11. Zeisberg, M., and Kalluri, R. (2004) *J. Mol. Med.* **82,** 175–181
12. Martinez-Hernandez, A., and Amenta, P. S. (1995) *FASEB J.* **9,** 1401–1410
13. Thiery, J. P. (2002) *Nat. Rev. Cancer* **2,** 442–454
14. Hay, E. D., and Zuk, A. (1995) *Am. J. Kidney Dis.* **26,** 678–690
15. Savagner, P. (2001) *Bioessays* **23,** 912–923
16. Peifer, M., and McEwen, D. G. (2002) *Cell* **109,** 271–274
17. Iwano, M., Plieth, D., Danoff, T. M., Xue, C., Okada, H., and Neilson, E. G. (2002) *J. Clin. Investig.* **110,** 341–350
18. Reichmann, E., Schwarz, H., Deiner, E. M., Leitner, I., Eilers, M., Berger, J., Busslinger, M., and Beug, H. (1992) *Cell* **71,** 1103–1116
19. Zeisberg, M., Hanai, J., Sugimoto, H., Mammoto, T., Charytan, D., Strutz, F., and Kalluri, R. (2003) *Nat. Med.* **9,** 964–968
20. Yang, J., and Liu, Y. (2002) *J. Am. Soc. Nephrol.* **13,** 96–107
21. Chagraoui, J., Lepage-Noll, A., Anjo, A., Uzan, G., and Charbord, P. (2003) *Blood* **101,** 2973–2982
22. Pagan, R., Martin, I., Llobera, M., and Vilaro, S. (1997) *Hepatology* **25,** 598–606
23. Postic, C., Shiota, M., Niswender, K. D., Jetton, T. L., Chen, Y., Moates, J. M., Shelton, K. D., Lindner, J., Cherrington, A. D., and Magnuson, M. A. (1999) *J. Biol. Chem.* **274,** 305–315
24. Mao, X., Fujiwara, Y., and Orkin, S. H. (1999) *Proc. Natl. Acad. Sci. U. S.A.* **96,** 5037–5042
25. Wang, Y. J., Li, M. D., Wang, Y. M., Ding, J., and Nie, Q. H. (1998) *World J. Gastroenterol.* **4,** 74–76
26. Zeisberg, M., Maeshima, Y., Mosterman, B., and Kalluri, R. (2002) *Am. J. Pathol.* **160,** 2001–2008
27. Zeisberg, M., Bonner, G., Maeshima, Y., Colorado, P., Muller, G. A., Strutz, F., and Kalluri, R. (2001) *Am. J. Pathol.* **159,** 1313–1321
28. Kovalovich, K., DeAngelis, R. A., Li, W., Furth, E. E., Ciliberto, G., and Taub, R. (2000) *Hepatology* **31,** 149–159
29. Zeisberg, M., Bottiglio, C., Kumar, N., Maeshima, Y., Strutz, F., Muller, G. A., and Kalluri, R. (2003) *Am. J. Physiol.* **285,** F1060–F1067
30. Takemoto, M., Egashira, K., Tomita, H., Usui, M., Okamoto, H., Kitabatake, A., Shimokawa, H., Sueishi, K., and Takeshita, A. (1997) *Hypertension* **30,** 1621–1627
31. Strutz, F., Okada, H., Lo, C. W., Danoff, T., Carone, R. L., Tomaszewski, J. E., and Neilson, E. G. (1995) *J. Cell Biol.* **130,** 393–405
32. Zeisberg, M., Khurana, M., Rao, V. H., Cosgrove, D., Rougier, J. P., Werner, M. C., Shield, C. F., Werb, Z., and Kalluri, R. (2006) *PLoS Med.* **3,** e100
33. Zeisberg, E. M., Ma, Q., Juraszek, A. L., Moses, K., Schwartz, R. J., Izumo, S., and Pu, W. T. (2005) *J. Clin. Investig.* **115,** 1522–1531
34. Bissell, D. M. (1998) *J. Gastroenterol.* **33,** 295–302
35. Kalluri, R., and Zeisberg, M. (2006) *Nat. Rev. Cancer* **6,** 392–401
36. Okada, H., Inoue, T., Kanno, Y., Kobayashi, T., Ban, S., Kalluri, R., and Suzuki, H. (2001) *Kidney Int.* **60,** 597–606
37. Bissell, D. M., Roulot, D., and George, J. (2001) *Hepatology* **34,** 859–867
38. Canbay, A., Higuchi, H., Bronk, S. F., Taniai, M., Sebo, T. J., and Gores, G. J. (2002) *Gastroenterology* **123,** 1323–1330
39. Miettinen, P. J., Ebner, R., Lopez, A. R., and Derynck, R. (1994) *J. Cell Biol.* **127,** 2021–2036
40. Bhowmick, N. A., Ghiassi, M., Bakin, A., Aakre, M., Lundquist, C. A.,

Engel, M. E., Arteaga, C. L., and Moses, H. L. (2001) *Mol. Biol. Cell* **12,** 27–36
41. George, J., Roulot, D., Koteliansky, V. E., and Bissell, D. M. (1999) *Proc. Natl. Acad. Sci. U. S. A.* **96,** 12719–12724
42. Sappino, A. P., Schurch, W., and Gabbiani, G. (1990) *Lab. Investig.* **63,** 144–161
43. Michalopoulos, G. K., and DeFrances, M. C. (1997) *Science* **276,** 60–66
44. Yang, C., Zeisberg, M., Mosterman, B., Sudhakar, A., Yerramalla, U., Holthaus, K., Xu, L., Eng, F., Afdhal, N., and Kalluri, R. (2003) *Gastroenterology* **124,** 147–159
45. Haase, V. H., Glickman, J. N., Socolovsky, M., and Jaenisch, R. (2001) *Proc. Natl. Acad. Sci. U. S. A.* **98,** 1583–1588
46. Duncan, S. A., and Watt, A. J. (2001) *Genes Dev.* **15,** 1879–1884
47. Heldin, C. H., Miyazono, K., and ten Dijke, P. (1997) *Nature* **390,** 465–471
48. ten Dijke, P., Korchynskyi, O., Valdimarsdottir, G., and Goumans, M. J. (2003) *Mol. Cell. Endocrinol.* **211,** 105–113
49. Friedman, S. L. (1999) *Semin Liver Dis.* **19,** 129–140
50. Gressner, A. M., and Bachem, M. G. (1990) *Semin. Liver Dis.* **10,** 30–46
51. Sugimoto, H., Yang, C., LeBleu, V. S., Soubasakos, M. A., Giraldo, M., Zeisberg, M., and Kalluri, R. (2007) *FASEB J.* **21,** 256–264

Molecular Basis of Cell and Developmental Biology:

Fibroblasts Derive from Hepatocytes in Liver Fibrosis via Epithelial to Mesenchymal Transition

Michael Zeisberg, Changqing Yang, Margot Martino, Michael B. Duncan, Florian Rieder, Harikrishna Tanjore and Raghu Kalluri

J. Biol. Chem. 2007, 282:23337-23347.
doi: 10.1074/jbc.M700194200 originally published online June 11, 2007